Received: 22 February 2022 | Revised: 13 June 2022 | Accepted: 9 September 2022

DOI: 10.1002/stc.3102

RESEARCH ARTICLE

WILEY

Real-time corrosion monitoring of an ultra-high performance fibre-reinforced concrete offshore raft by using an autonomous sensor system

José E. Ramón[1] | **José M. Gandía-Romero**[2] | **Román Bataller**[3] | **Juan A. López**[4] | **Manuel Valcuende**[5] | **Juan Soto**[2]

[1]Instituto de Ciencias de la Construcción Eduardo Torroja, CSIC, Madrid, Spain

[2]Interuniversity Research Institute for Molecular Recognition and Technological Development, Universitat Politècnica de València, Universitat de València, Valencia, Spain

[3]Chatu Tech S.L., Terrassa, Spain

[4]Research & Development Concretes S.L., Valencia, Spain

[5]Department of Architectural Construction, Universitat Politècnica de València, Valencia, Spain

Correspondence
José M. Gandía-Romero, Interuniversity Research Institute for Molecular Recognition and Technological Development, Universitat Politècnica de València, Universitat de València, Camino de Vera s/n, 46022 Valencia, Spain.
Email: joganro@csa.upv.es

Funding information
UPV, Grant/Award Number: SP20180245; Spanish Ministry of Economy and Competitiveness, Grant/Award Numbers: BIA2016-78460-C3-3-R, PID2020-119744RB-C21, PID2020-119744RB-C22; Spanish Ministry of Science and Innovation, Grant/Award Number: FPU13/00911

Summary

The excellent high-durability features of ultra-high performance fibre-reinforced concrete (UHPFRC) have been verified in laboratory studies, but its performance under service conditions are being studied. Indeed, structural health monitoring (SHM) can be considered an efficient strategy to assess built structures in which concrete matrix performance differs from that those found when assessing laboratory samples (variable actions, cracking, etc.). This work presents INESSCOM, an automated corrosion rate monitoring system, as an innovative support to SHM strategy to monitor UHPFRC structures in terms of durability. Its innovation lies in its durable and multi-parametric sensor designed to be embedded in multiple parts of a structure. The results from previous laboratory tests and those obtained during real-time monitoring of an offshore UHPFRC raft are presented. Acceptable deviation of 20% was obtained in corrosion rate measurements with the advantageous reference-electrode-free cell of the sensor with respect to the classical three-electrode cell. Furthermore, sensor provided accurate corrosion measurements in UHPFRC despite its extremely high electrical resistivity and large amount of steel fibres. After 17-month monitoring of the UHPFRC raft, excellent performance was evidenced under service conditions with corrosion rate values always <0.1 μA/cm^2. Conversely, corrosion rate reached 0.4 μA/cm^2 in a conventional concrete specimen installed for comparison. Corrosion initiation and propagation stages were clearly defined through the corrosion-penetration-damage (μm) diagram obtained for the specimen. Present work positions INESSCOM as an innovative support to structural health monitoring strategy in UHPFRC structures.

KEYWORDS

durability, non-destructive technique, sensor, steel corrosion, structural health monitoring, ultra-high-performance fibre-reinforced concrete

1 | INTRODUCTION

Ultra-high performance fibre-reinforced concrete (UHPFRC) is a cement-based composite material. It combines three technical advances in concrete: (1) high compressive strength, (2) ductile behaviour under tension due to the presence of steel fibres and (3) special selection of fine and ultrafine aggregates, which leads to dense particle packing, high durability and flowability.[1] The performance of ultra-high performance concretes (UHPC) and ultra-high fibre-reinforced concretes (UHPFRC) for durability aspects is excellent compared with conventional concretes (CC) or even high performance concretes (HPC). In the last 20 years, besides lack of standards and regulations, which has been an obstacle for their development to a certain extent, interest in such concretes has provided real-scale examples in many countries.[2]

Therefore, excellent UHPFRC performance makes it an interesting alternative for extending the lifespan of concrete structures. Although good UHPFRC performance has been demonstrated under laboratory conditions,[3] its performance under real service conditions must be studied in-depth. This makes analysing the mid- and long-term evolution of durability indicators on real structures worthwhile. In line with this, structural health monitoring (SHM) is an extremely useful strategy because it was conceived to follow up the key parameters for durability assessment, continuously and in real time. Knowledge of materials under service conditions is key because it allows the durability strategy to be followed to be defined more accurately and to also deal with possible deterioration problems in the built structure well in advance.

It is well known that one of the factors that most affects the durability of concrete structures is rebar corrosion. It is worth using non-destructive tools capable of on-site monitoring the corrosion condition of the reinforcement. Along these lines, in recent decades, different monitoring techniques and methods have been developed using different technologies. Towards the end of the 1970s, reference embedded electrodes started being used to monitor the corrosion potential of the reinforcement.[4] Despite this method being quite fast and direct, the corrosion potential is a qualitative parameter, since it only provides an estimation of the corrosion risk of the rebars.[5] Consequently, in recent decades, much effort has been made to incorporate into SHM those systems capable of providing quantitative information about steel corrosion that would, therefore, be more useful for predicting the service life of structures and establishing more suitable prevention and/or maintenance strategies.

The corrosion level of the reinforcement is determined from the corrosion rate (V_{CORR}) value, typically expressed in terms of current density (i_{CORR}) according to Andrade and Alonso.[6] Corrosion rate is a very useful parameter in service life prediction, since reference concrete standards as the EN 1992 Eurocode 2[7] are using it to determine the remaining service life of the structure once corrosion has been initiated, that is, the extent of the propagation period (t_P) in the Tutti's model.[8] A representative value of i_{CORR} or V_{CORR} is required in lifespan assessment models, that is, an average value along certain time (usually a year) with enough frequency (at least four measurements, one in each season).[6]

The most widespread systems determine the corrosion rate of the reinforcement by the electrochemical polarisation of a sensor embedded close to rebars.[9] To this end, this sensor requires a 3-electrode setup formed by (a) a working electrode (WE) manufactured with a piece of carbon steel with a similar composition to rebars; (b) a counter-electrode (CE), normally made of stainless steel; and (c) a reference electrode (RE), generally of the MMO type. Using the RE can imply reliability issues because the long-term electrochemical stability of available RE electrodes cannot always be guaranteed, especially if embedded REs are used as their maintenance cannot be performed.[10] Another possible limitation with conventional corrosion sensors is for corrosion macrocells to appear between areas of the structure with different electrochemical potentials, which is often the case in practice.[11] As the WE is an isolated element, it does not participate in macrocell processes, and consequently, the corrosion rate measurement might not be representative of the actual condition of the reinforcement in the sensor-monitored area.[12]

Furthermore, some systems exist that employ more advanced technology. Some proposals involve optical sensing technology-based sensors,[13] whose capacity to be miniaturised stands out, and inductively coupled magnetic fields-based sensors[14] that can be tested wirelessly, which greatly facilitates their field implementation. Also, techniques based on acoustic emission[15] and guided ultrasonic waves[16] have proven effective in identifying corrosion damage in reinforced concrete. To date however, the information provided by such systems is limited to estimates of whether rebars are in the passive or active state. This could make the early detection of corrosion processes and, consequently, the planning of efficient intervention strategies, difficult.

In practice, performing onsite and continuous corrosion monitoring by means of portable sensors is a complex and high-cost task that also requires specialised labour. This is a key aspect, hence the ever-growing interest shown in developing smart sensor systems capable of real-time and remote monitoring the corrosion state of structures. In practice, the success of these sensor systems within the SHM strategies is due to the use of long-term reliable, affordable and

easy-to-install technology.[17] The most recent works have focused on improving these sensor systems by incorporating wireless technology[18] because this not only facilitates their field installation but also represents considerable progress into incorporating reinforced concrete structures into the prevailing Internet of Things (IoT) paradigm.[19] The next challenge is to implement intelligent algorithm-based and deep learning-based damage identification methods in next-generation structural health monitoring systems.[20,21]

The system employed in the present research work was INESSCOM (Integrated Network of Sensors for Smart Corrosion Monitoring). It is a smart system of embedded sensors that has been developed and patented by researchers from the Universitat Politècnica de València[22,23] to remotely monitor corrosion rate in multiple structure areas by applying an innovative measurement method.[24,25] INESSCOM provided the basis for the development of the Corrochip© sensor system from Witeklab. One highlighted use was to monitor an offshore raft manufactured with UHPFRC by the company Research & Development Concretes S.L. as part of the European Project SME INSTRUMENT (SELMUS-738777). This type of structures is exposed to extreme durability conditions because, apart from the marked aggressive nature of the marine environment, we must also consider distortions caused by waves, plus service loads. Under such severe conditions, UHPFRC is presented as a material capable of ensuring the durability of these marine structures, which must be assessed by SHM strategies. Nonetheless, UHPFRC has some very particular characteristics, such as an extremely high electrical resistivity and large amounts of steel fibres, which can pose a challenge when performing electrochemical measurements by means embedded sensor.

The present work aimed to demonstrate INESSCOM's reliability to monitor corrosion processes in floating UHPFRC structures under service conditions. Interest lies in being able, for the first time, to remotely and real-time monitor UHPFRC corrosion rate along with additional parameters, such as electrical resistance, in at least the medium term. Before on-site implementation, the innovative measurement protocol of the embedded sensor used in the monitoring system was validated using laboratory scaled-down concrete specimens. After 17 months of raft monitoring, the results obtained by the sensor system at four different points of the structure, were analysed and compared to the results obtained from a conventional concrete sample that was installed in the raft itself while to be exposed to exactly the same environmental conditions as the UHPFRC. In both cases, UHPFRC and conventional concrete, INESSCOM was intended to provide accurate corrosion rate assessment, which, in the case of the UHPFRC structures, is a demanded novelty for lifespan prediction.

2 | EXPERIMENTAL SETUP

2.1 | Materials

The ultra-high performance fibre-reinforced concrete (UHPFRC) Formex® is the subject of this study, whose patent to manufacture certain specific designs is used by the company PREFFOR. This UHPFRC incorporates a 2% in volume of 17-mm length steel fibres with a slenderness ratio of 68 and has the water/binder ratio of 0.2. The 28-day compressive and the tensile strengths obtained in 100-mm cubic specimens were 135 and 6 MPa, respectively.

Due to the well-known high durability performance of the UHPFRC, it is assumed that significant corrosion rates will not be achieved in the medium term. Thus, a conventional concrete (CC) with the high water/cement ratio of 0.6 and the 28-day compressive strength of 36 MPa was made for comparison purposes. The composition of the CC was 300 kg/m^3 of Portland cement CEM-I 42.5 R-SR, 1265 kg/m^3 of sand 0/4 (fine aggregate), 713 kg/m^3 of gravel 4/12 (coarse aggregate), 178 kg/m^3 of water and 2.8 kg/m^3 of polycarboxylate-based superplasticizer (Viscocrete 3425).

The CC is not intended to be used in the raft manufacturing, as is the case of the UHPFRC Formex®, since we are aware that its quality is inadequate to ensure passivity of the reinforcement in the severe marine environment. The CC is intended to obtain, within a reasonable period of time, significant corrosion rates clearly different from those obtained in the UHPFRC, thus facilitating the validation of the INESSCOM sensor system.

2.2 | The UHPFRC raft

This offshore raft is a floating structure made up of a frame of prestressed UHPFRC beams on which wooden joists are supported to fasten the ropes for mussel farming. These structures are currently prefabricated by the company Preffor, with are licensed with the patent of Research & Development Concretes S.L. (RDC). The employed concrete was the

UHPFRC previously described in Section 2.1. The prefabricated elements were produced in València and transported by road on a special truck to O Grove (Pontevedra, Spain). There the Offshore raft was assembled in the port to be later launched towards the Arousa estuary (Pontevedra, Spain). as Figure 1 shows.

Figure 1a shows the complete offshore raft scheme, whose design is similar to traditional wooden ones. It is rectangular, measures 20 × 27 m (540 m^2) and weights 53 T. Its structure is supported on six steel floaters coated with glass fibre-reinforced plastic. The six main beams, each measuring 20 m long, were arranged into pairs and supported on two floaters. Eleven secondary beams were laid perpendicularly on the main beams and measured 27 m long, which, in turn, supported the 34 lines of wooden beams.

The distance between both the main and secondary beams and the water surface was not constant in time, since it depended on the mussel weight hanging on the raft. Distance from the water surface varied between −5 and 60 cm for main beams and between 17 and 83 cm for secondary beams. Therefore, raft beams are considered to be in the tidal, splash and spray conditions in marine environment, corresponding to the XS3 exposure class of the European standard EN 206.[26]

2.3 | The corrosion monitoring system

The corrosion measuring system employed to monitor the UHPFRC raft was INESSCOM (Integrated Network of Sensors for Smart Corrosion Monitoring). It was conceived as an autonomous monitoring system that is permanently installed in a structure to periodically and simultaneously evaluate corrosion at different control points (CPs).[12,23] At each CP, corrosion rate is measured by embedded sensors. The data acquired at the CPs are collected and processed by a central module whereby the structure's state can be remotely consulted in real time.

INESSCOM was installed in the offshore raft to monitor reinforcement corrosion at five CPs according to the scheme shown in Figure 2a. These CPs were selected with the aim to obtain the most valuable information as possible in accordance with economic resources available for monitoring. Four of the CPs are located on the UHPFRC beams (Figure 2b), two of them on main beams (CP1 and CP2) and the other two on secondary beams (CP3 and CP4). These CPs (CP1–CP4) were strategically positioned near the floaters, where bending forces were expected to be the highest. CP5 is located on a control sample (15 × 25 × 7 cm) made with the conventional concrete (CC) previously described in Section 2.1 (Figure 2c). It must be recalled that the present work aims to evaluate the in-service durability of the UHPFRC used in the raft. The aim of using this sample is to have a well-differentiated steel-concrete system in relation to the raft UHPFRC for comparison purposes as the specimen was intended to be potentially more susceptible to suffering corrosion. The CC specimen was designed with smaller dimensions than the UHPFRC beams with the aim of not interfere with normal mussel-farming tasks carried out in the raft.

At each CP, corrosion measurements are performed by means of an embedded sensor (Figure 3), which is polarised by a specially designed measuring device (Figure 4d). Detailed information about the corrosion sensor and its operative principle is described below in Section 2.3.1. The central module, shown in Figure 2e,f, consists on a Raspberry Pi (RPi)

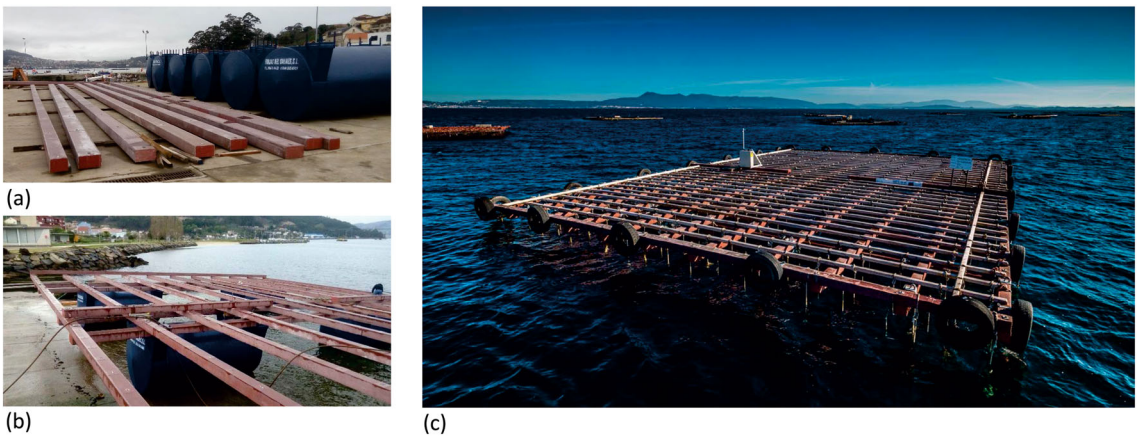

FIGURE 1 (a) UHPFRC beams (main and secondary) and floaters stored for assembling, (b) assembling process and (c) completely assembled offshore raft operating in the Arousa estuary (Pontevedra, Spain)

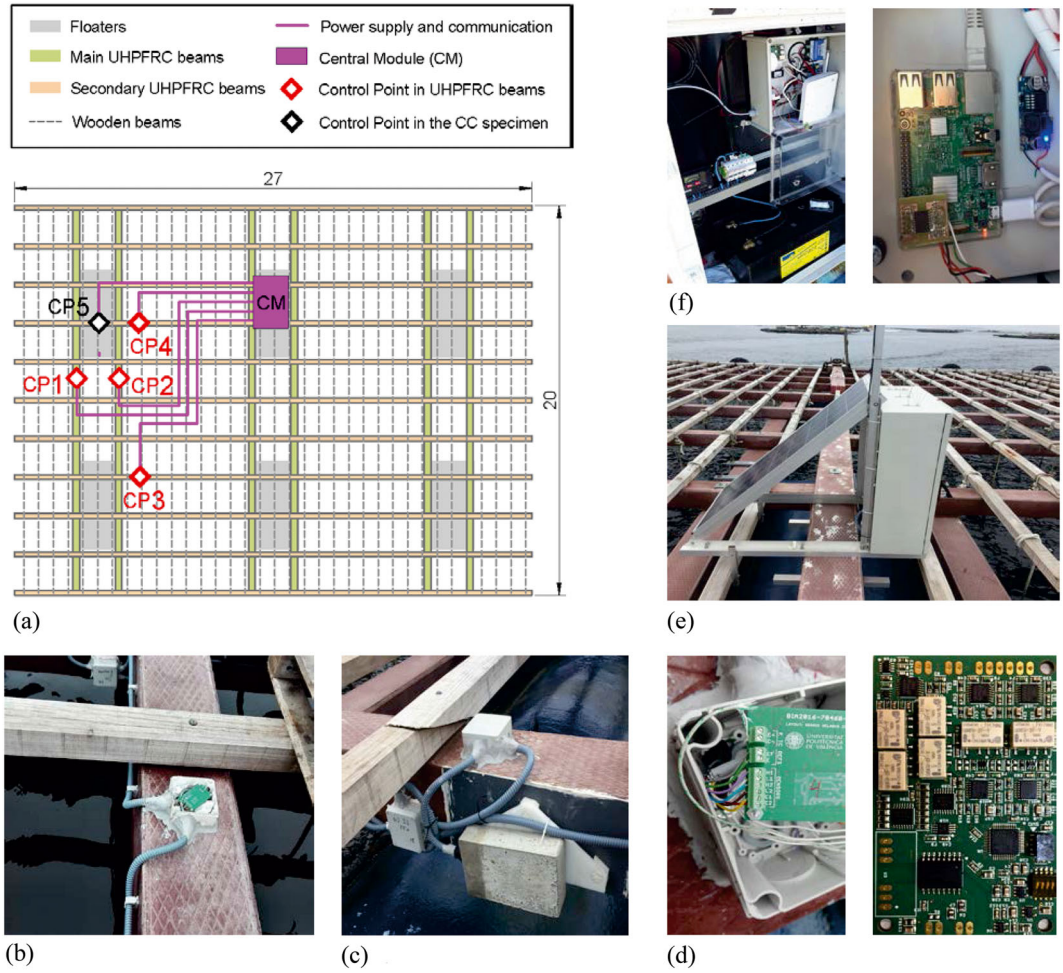

FIGURE 2 (a) Scheme of the offshore raft made of UHPFRC showing the main INESSCOM system components: (b) control points (CPs) on UHPFRC beams and (c) the CP on the conventional concrete sample, on which corrosion is measured with the (d) corresponding miniaturised electronic equipment connected to (e) the central module which, in apart from the solar photovoltaic power system, contains (f) the microPC that manages the system. Dimensions in metres

that is connected by an RS-485 bus with the measuring devices of the CPs to automatically launch the measurements and collect the results. The collected information is processed and interpreted in corrosion parameters of interest by a specific analysis code developed with R software. This allows information about the structure's condition to be updated and can be consulted remotely by means of the 4G Internet connection integrated into the central module.

All the system components, except the embedded sensors, were onsite installed after assembling the structure in the port. The elements employed to connect and distribute the electric wiring had a high level of protection. The measuring devices were set up in separate boxes close to their respective CPs (Figure 2b–d). Next to the RPi that manages the sensors network from the central module, a photovoltaic power supply system was placed, along with a 4G connection module, which was installed at an accessible point on the structure by the company Wireless Galicia S.L. (Figure 2e).

2.3.1 | Sensor design and manufacture

At each CP, the sensor allows to obtain corrosion rate through the electrochemical polarisation of a carbon steel working electrode (WE). Placing two WEs on each CP is useful (Figure 3a) because it allows two readings to be obtained in order to verify reproducibility of the measurement at each CP. To ensure representative measurements, WEs must be manufactured using the same steel as the reinforcement of the structure to be monitored. For the offshore raft, WEs were manufactured using a section of the 7-wire strand employed as reinforcement in the prestressed UHPFRC raft

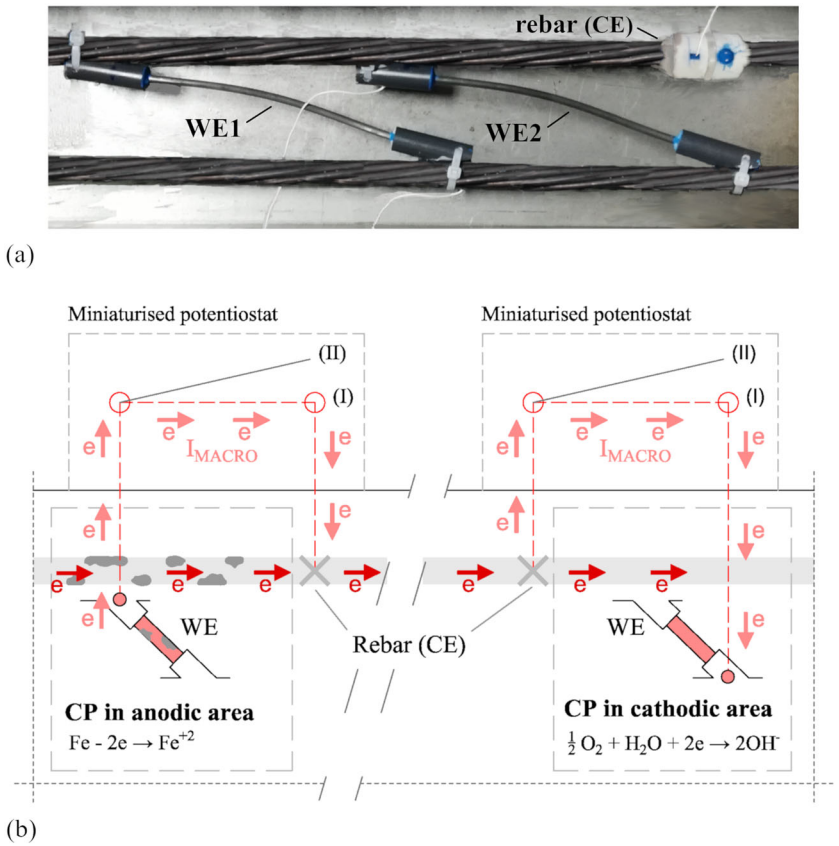

FIGURE 3 (a) Example of the corrosion sensor assembled in each CP of the UHPFRC raft before casting, which includes two WEs and reinforcement is used as CE. (b) Scheme of the corrosion measurement principle of the sensor showing its interaction with a macrocell depending on whether the CP is in the anodic or cathodic area. The sensor normally remains connected to the rebar (I) to participate in possible macrocell currents (I_{MACRO}) and is sporadically disconnected and isolated to take corrosion measurement (II).

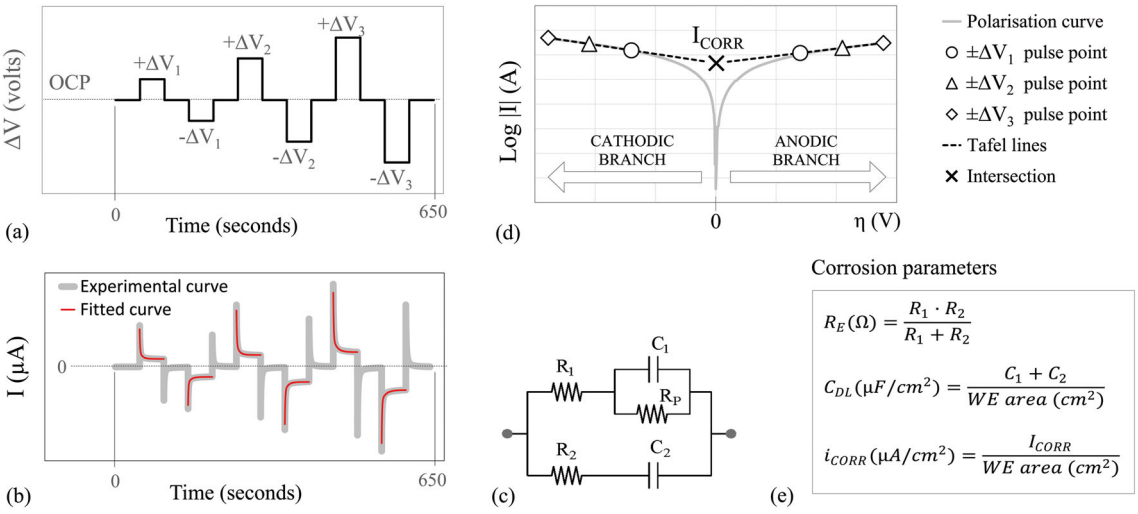

FIGURE 4 Scheme of the main processes of the PSV technique applied to measure corrosion in the embedded sensor: (a) the potentiostatic pulse sequence applied; (b) the experimental intensity-time curve obtained, which is fitted by using (c) an equivalent circuit; (d) Tafel lines determination and intersection to determine corrosion current; and (e) calculation of final corrosion parameters

beams. Specifically, one of the wires of 5 mm in diameter and 150 mm was used as WE, whose ends were encapsulated in an epoxy resin-filled PVC piece to delimit the working area and protect the electrical connection to the copper wire installed at one of the ends. The WEs used for the corrosion sensor validation in laboratory specimens were made from a section of the corrugated carbon steel bars employed as reinforcement of the specimens.

The use of small WEs as proposed here (150 mm in length) is the usual practice for local corrosion studies,[9] since the use of much larger electrodes could favour the appearance of internal corrosion macrocells at the WE,[27,28] which could cause that the measured corrosion rate not to be representative of the local CP. Moreover, if the electrode is much bigger, the applied overpotential cannot be controlled precisely because it requires a more complex electronic design of the measuring device. In each CP, the two WEs of the sensor were embedded at the same depth as the reinforcement, that is, 2 cm.

The corrosion sensor employs a 2-electrode cell to perform the measurements; that is, only the CE is required to polarise the WE. This 2-electrode configuration can be successfully applied when the CE area is substantially bigger than that of the WE.[23] This requirement is ensured when the reinforcement of the structure itself is used as CE, since the reinforcement area (cm^2) of the beam is between 11,000 (main beams) and 15,000 (secondary beams) times greater than that of the sensor WE. In order to perform measurements, a wire is connected to the CE and sealed with epoxy resin (Figure 4). This 2-electrode configuration eliminates the need for a RE. Despite MMO-type electrodes currently provide promising performance, suppressing the RE in the sensor is an obvious advantage, since the 2-electrode configuration results in a very robust sensor setup which facilitates its installation and favours its durability. Moreover, the corrosion sensor employed on the raft includes a type-K thermocouple to measure temperature inside concrete, since it is a parameter known to affect corrosion rate.

The different sensor components described above were installed at each CP of the raft after tensioning the strands before casting (Figure 3a). In order to avoid offering an easy way for oxygen and moisture to enter into the concrete elements, the sensor cabling runs inside the concrete element until reaching the measuring device, which was mounted into an outside box with IP 67 protection placed on the concrete surface and sealed with silane-terminated polymer. The sensor system described here is the result of a strategic design to ensure that its installation would not affect either the execution process or the in-service performance of the raft.

2.3.2 | Operational principle of the sensor

Figure 3b shows the operational principle of the corrosion sensor, in which envisages two sensor modes: (I) the connected mode and (II) the test mode.

Connected mode (I)

In mode I, the sensor's WEs remain electrically connected to the rebars, that is, the CE. In this situation, the corrosion condition of the WE will be very similar to that of the reinforcement (CE) in the CP region, since both electrodes (i) are made of the same material, (ii) are under the same physico-chemical local conditions (oxygen availability, pH, humidity, presence of aggressive anions, temperature, etc.) and (iii), something unusual in common corrosion sensors, are under the same macrocell corrosion kinetics. Thus, the sensor will be involved in possible macrocells by providing a macrocell current (I_{MACRO}) proportional and of the same sign to that provided by the adjacent rebars to which the WE is connected (Figure 3b).

Test mode (II)

Whenever corrosion rate must be determined, the sensor goes into mode II. In this situation, the sensor WEs are temporarily disconnected from the reinforcement, which then acts as a CE in the 2-electrode measuring cell required to apply the electrochemical polarisation technique. The technique employed consist on an innovative approach of the potential step voltammetry (PSV), which is described in detail in previous works[25] and whose main processes are found in the scheme shown in Figure 4. The PSV technique bases the corrosion density (i_{CORR}) measurement on the Tafel intersection method but offers the advantage of Tafel lines being obtained much more quickly and, most important, without risk of producing the irreversible polarisation of rebars.

As shown in Figure 4d, each Tafel line is defined by three points on the polarisation curve. Each point results from the application of a 50-s potentiostatic pulse (ΔV), so for each line, three pulses of different amplitude are applied: $\pm\Delta V_1$, $\pm\Delta V_2$ and $\pm\Delta V_3$. These potential steps are included in the sequence: $OCP/+\Delta V_1/OCP/-\Delta V_1/OCP/+\Delta V_2/OCP/$

$-\Delta V_2/OCP/+\Delta V_3/OCP/-\Delta V_3/OCP$. As can be seen in Figure 4a, it is a symmetrical sequence that alternates anodic and cathodic steps with the inclusion of zero-amplitude steps between them in order to return the steel-concrete system to its original state, that is, its original open circuit potential (OCP). In this way, the charge that accumulates during testing considerably reduces compared with the classic sweep voltammetry technique typically used in classic Tafel intersection method. Consequently, the irreversible polarisation risk of the WE is reduced with the use of PSV, as previous work demonstrates.[25]

The OCP corresponds to the WE potential measured before polarisation versus the reference electrode (RE). Nevertheless, in the 2-electrode configuration employed in the sensor, the OCP is the WE potential measured versus the CE. As the surface of the CE (reinforcement) is much higher than that of the WE, no significant potential variation, and therefore, no polarisation of the CE will occur during the measurement. Therefore, the CE is here used as a pseudo-reference to determine the OCP.

Each point on Tafel lines (Figure 4d) is obtained by modelling the system's transitory response to the respective ΔV pulse (Figure 4b) with the equivalent circuit shown in Figure 4c, whose theoretical basis is found in a previous work.[24] The circuit components are calculated by minimum squares fitting of the current-time response. This allows the faradaic current (I_F) that passes through the system to be determined as $I_F = \Delta V/(R_1 + R_P)$ and corresponds to the ordinate of each point on Tafel lines (Figure 4d). The abscissa is the overpotential (η) applied to the respective step and is obtained as $\eta = \Delta V - (I_F \cdot R_E)$. Parameter R_E is the electric resistance of concrete, which, along with double-layer capacity (C_{DL}), is calculated from the circuit components as shown in Figure 4e. Once both Tafel lines (anodic and cathodic) are built, corrosion current is obtained (I_{CORR}) (Figure 4d) from their intersection and is used to calculate the corrosion current density (i_{CORR}) (Figure 4e).

2.4 | Validation tests

The reliability of the embedded corrosion sensors included in the INESSCOM system (Section 2.3.1) was studied in concrete specimens.

2.4.1 | Two-electrode measuring cell

The reliability of the 2-electrode measuring cell of the sensor employed in INESSCOM was studied for the corrosion rate measurement by the PSV technique. The results obtained with this configuration were compared with those obtained when the PSV was applied with a conventional 3-electrode cell. It should be noted that the reliability of PSV with a 3-electrode cell was validated against reference methods previously.[25]

Validation of the 2-electrode cell was here performed using reinforced concrete specimens with different corrosion level. These specimens were three slabs (slab-1, slab-2 and slab-3) of 50 × 50 × 10 cm in size using the conventional concrete (CC) described in Section 2.1. Specimens were subjected to well-differentiated corrosion processes:

- Slab-1: chloride-induced corrosion
- Slab-2: carbonation-induced corrosion
- Slab-3: in absence of depassivating ions, non-aggressive environment.

Chloride and carbonation were selected to represent the two most frequent causes of reinforcement corrosion. Slab-1 was chloride contaminated by mixing a 4% of chlorides per weight of cement using NaCl. The three specimens were demoulded 24 h after casting and were kept inside a curing chamber at 100% relative humidity and a temperature of 20 ± 1°C for 28 days. After this period, slab-1 and slab-3 were kept under laboratory conditions, while slab-2 was placed inside a carbonation chamber with 5% carbon dioxide at 65% relative humidity for 74 days. At this point the carbonation depth obtained from the phenolphthalein test in 100 mm concrete prisms was higher than the cover depth of the slab.

Each slab was considered to be a CP to be monitored with the INESSCOM system. For this purpose, all the components described in Section 2.3 were installed. As seen in Figure 5, a corrosion sensor was embedded in each specimen as described in Section 2.3.1. The sensor was manufactured with a corrugated bar of 8 mm in diameter, which was composed of three WE with an exposed area (S_{WE}) of 18.9 cm^2 and a CE with an exposed area (S_{CE}) of 820.5 cm^2. This

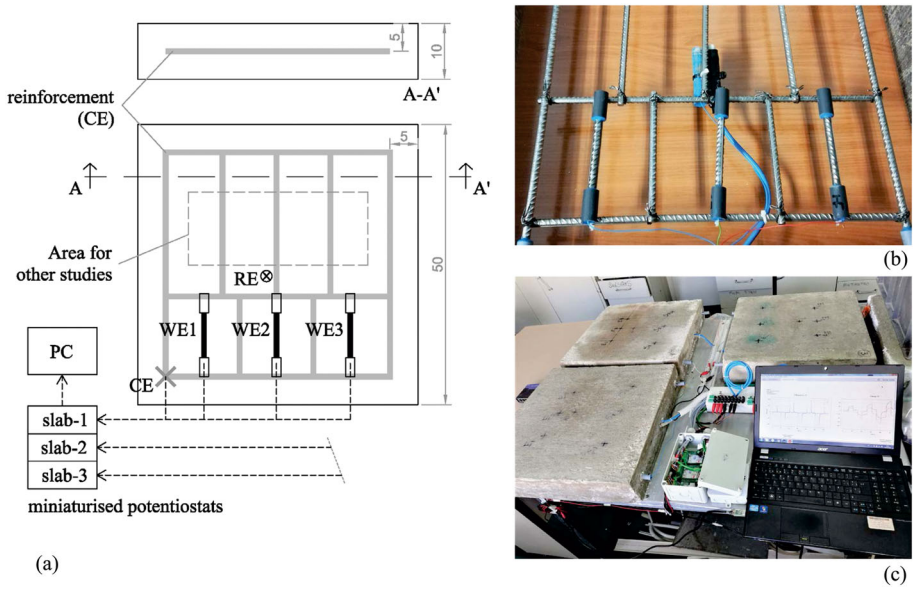

FIGURE 5 (a) Scheme of the concrete slab used for the 2-electrode PSV measurement validation showing the INESSCOM components employed (dimensions in centimetres); (b) installation of the three WEs and the CE that make up the corrosion sensor, along with the model ERE 20 manganese dioxide reference electrode (RE); (c) the measuring system completely assembled in the slabs

results in a S_{CE}/S_{WE} ratio of 43.4 which, according to previous works,[23] enables to perform corrosion measurements with the 2-electrode (WE/CE) cell. To validate this cell, an embedded RE was incorporated into the specimens, which was the model ERE 20 manganese dioxide electrode (MnO_2) from FORCE Technology, thereby enabling a 3-electrode measuring cell (WE/RE/CE) be used as a reference in the validation.

The PSV measurements with the 2-electrode cell were applied by using the electronic measuring device included in the INESSCOM system, while the 3-electrode measurements were applied by using the PGSTAT 100 potentiostat from Metrohm Autolab. Validation measurements were performed at laboratory temperature ($20 \pm 2°C$) in two different phases: first under ambient relative humidity (≈60%) and second under high relative humidity (≈100%) by covering the slabs with damp cloths to favour steel corrosion.

2.4.2 | Sensor response in UHPFRC

The sensor system's capacity to perform corrosion rate measurements in UHPFRC was studied. Corrosion monitoring this type of concrete poses a significant challenge due to its very low porosity and the presence of steel fibres in its matrix.

For that purpose, a prism specimen of $25 \times 15 \times 13$ cm in size was built with an embedded sensor composed of two WEs and a CE manufactured with corrugated steel bars of 10 mm and 12 mm in diameter, respectively. A scheme of the specimen is found in Figure 6a. For comparison purpose, two twinned samples were manufactured (Figure 6b): one with the UHPFRC used in the offshore raft and another with the conventional concrete (CC), both described in Section 2.1.

The PSV measurements were periodically performed on these specimens by using the sensor with the 2-electrode cell (as normally used in INESSCOM) for 5 months in the laboratory at room temperature ($20 \pm 2°C$). During this period, resistivity was also measured in 100 mm prism samples by using the direct method described in literature[29] with a Crison GLP 32 conductivity-meter.

3 | RESULTS AND DISCUSSION

3.1 | Corrosion sensor reliability

This section presents the results obtained while validating the INESSCOM sensor system employed to monitor the UHPFRC raft.

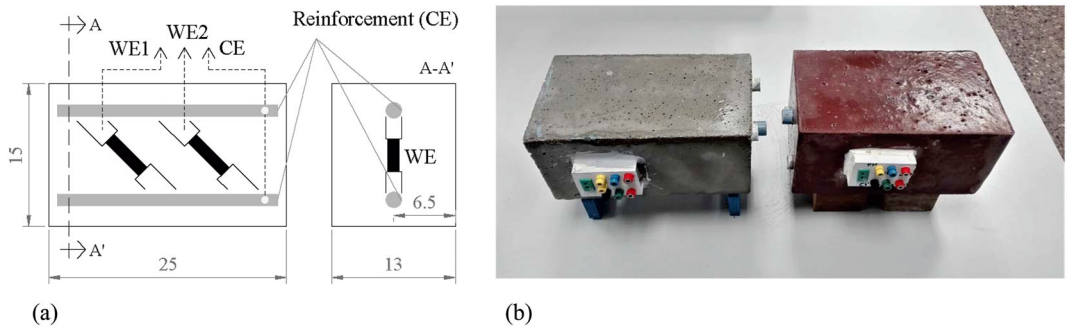

FIGURE 6 (a) Scheme of the concrete sample used to evaluate the corrosion sensor's response in UHPFRC. (b) Two twinned specimens were manufactured: one using the UHPFRC Formex® (right) and another using the conventional concrete (CC) (left). Dimensions are expressed in centimetres.

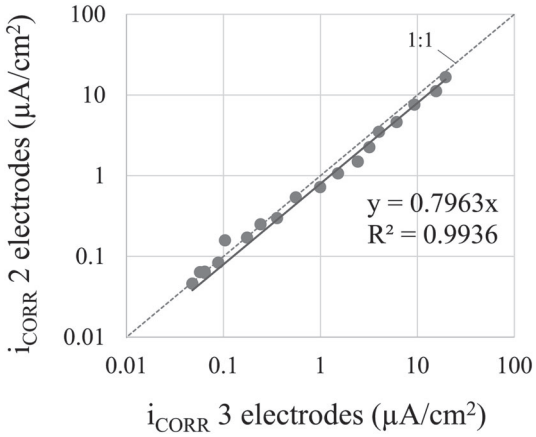

FIGURE 7 Comparison of the corrosion current density (i_{CORR}) obtained with the PSV technique by using the 2-electrode cell and the 3-electrode cell in the INESSCOM sensor

3.1.1 | Validation of the 2-electrode measuring cell

The reliability of the 2-electrode cell used by the sensor to perform corrosion rate measurements was analysed. Figure 7 compares the i_{CORR} results obtained with the 2-electrode cell to those obtained with the classic 3-electrode cell, both employing the PSV technique. The slope of the regression line is 0.7963, which indicates that the 2-electrode cell tends to underestimate i_{CORR} by about 20% in relation to the 3-electrode cell. Previous works report similar deviations when comparing reference techniques such as Linear Polarisation Resistance and Tafel Extrapolation methods.[25] It should be noted that the corrosion level ranges associated with i_{CORR} are based on a logarithmic scale[6,30]; thus, the deviation observed with the 2-electrode cell does not introduces significant errors in the estimation of the corrosion condition of the reinforcement. In any case, these differences become even less important given the possible improved long-term reliability in INESSCOM associated with the use of the 2-electrode setup as sustained in Section 2.3.1.

3.1.2 | Sensor response in UHPFRC

This section studies the sensor ability to perform corrosion rate measurements in UHPFRC by using the 2-electrode cell previously validated in Section 3.1.1. Figure 8a shows a comparison of the i_{CORR} value monitored in the UHPFRC specimen and in the conventional concrete (CC) specimen. Initially, i_{CORR} was between 0.080 and 0.140 µA/cm^2, which are slightly higher values associated with the passive layer formation period.[31] After these first days, a swift downward trend towards extremely low and stable i_{CORR} values (bellow 0.010 µA/cm^2) was accurately recorded in the UHPFRC specimen with the two working electrodes (WE1 and WE2) of the sensor. In the CC specimen, the i_{CORR} was also

accurately and reproducibly measured with the sensor, whose downward trend was less marked and clearly distinct from that of UHPFRC and tended to stabilise at around 0.040 μA/cm^2 towards the end of the period.

Differences in the i_{CORR} trend discussed above for both concretes can be associated with concrete resistivity results shown in Figure 8b, since an inversely proportional relationship between resistivity and reinforcement corrosion rate has been described elsewhere.[32,33] Initially, resistivity was lower in both concretes due to higher water availability during the first few days of the curing period, and, therefore, steel corrosion was favoured at this stage (i_{CORR} was similarly high in both concretes). As concrete hydration proceeded, the passive film was gradually being consolidated and water availability was being reduced, apparently more steeply in the UHPFRC specimen as reflected in the monitored resistivity. That is probably due to the high cement content in the UHPFRC. Resistivity results would explain the differences between the i_{CORR} trend of both concretes. Towards the end of the period, the resistivity of the CC specimen reached around 100 kΩ·cm, which is precisely the threshold above which the corrosion risk is considered negligible.[29] In the case of the UHPFRC, resistivity was well above this limit, that is, around 450 kΩ·cm, which is approximately 4.5 times higher than those of the CC. This order of magnitude looks very close to that observed in the i_{CORR} comparison, but in reverse order (Figure 8).

In short, both CC and UHPFRC specimens are clearly in the passive state, although there is a clear difference in the i_{CORR} value (Figure 8a) as a result of the cement matrix porosity (Figure 8b). In the case of the UHPFRC, its high compactness seriously impedes the diffusion of depassivating ions. In previous work,[34] a complete characterisation of the UHPFRC used was performed, obtaining chloride migration and capillary suction coefficients typical of high durability concretes. Therefore, the main way for aggressive agents to penetrate into UHPFRC reinforcement and trigger corrosion would be if the concrete cover is cracked. However, no cracks have been observed in any of the specimens studied here.

The higher porosity of the CC specimen can be inferred from the resistivity results shown in Figure 8b, so it could be considered that the humidity and oxygen availability is also higher. This would explain why, even in the passive state, corrosion rate is higher in the CC ($i_{CORR} \approx 0.040$ μA/cm^2) than in the UHPFRC ($i_{CORR} \approx 0.010$ μA/cm^2). Although the very low gas permeability coefficient found in previous study[34] for the UHPFRC used, the little available oxygen could be sufficient to feed the cathodic semi-reaction of the corrosion process, since corrosion occurs slowly ($i_{CORR} \approx 0.01$ μA/cm^2). If the oxygen concentration were insufficient, the cathodic semi-reaction could be being fed by the reduction of the Fe(III)-oxides in the passive layer. Under this hypothesis, the anodic semi-reaction would consist on the oxidation of the Fe(II)-oxides in the passive layer. This hypothetical redox process proposed could be any, or a combination of, the following:

$$2Fe_3O_4 + 2OH^- \leftrightarrow 3\gamma - Fe_2O_3 + H_2O + 2e^- \quad (1)$$

$$Fe_3O_4 + OH^- + H_2O \leftrightarrow 3\alpha - FeOOH + e^- \quad (2)$$

Although it is assumed that in the UHPFRC the water is mostly combined in the hydrates, the Van der Waals-type bonding forces that generally retain the H_2O molecules would not pose a great impediment to their dissociation, even

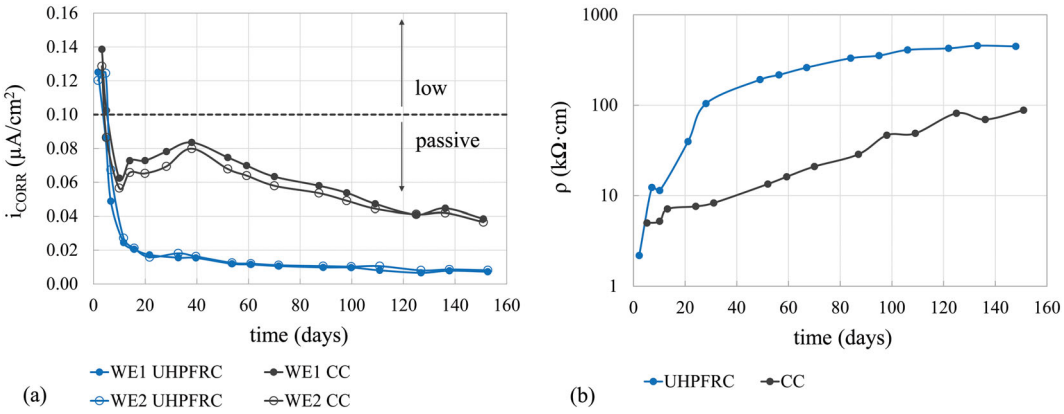

FIGURE 8 (a) Corrosion density (i_{CORR}) follow-up in the UHPFRC and conventional concrete (CC) specimens with the INESSCOM corrosion sensor and (b) resistivity evolution (ρ) measured by the direct method in prismatic specimens (4 × 4 × 16 cm) during the same period for both concrete types

on a transitional basis, forming the OH^- anions and H^+ (protons) required to neutralise the excess charge of the redox process (Equations (1) and (2)).

Furthermore, it could be argued that metallic fibres are the electron transfer path during the redox process. However, over a certain UHPFRC volume, fibres tend to appear randomly oriented and cement-coated. If not, it would be difficult to explain the high resistivity values recorded for the UHPFRC (Figure 8b). Therefore, fibres would offer higher electrical resistance than the rebar, therefore, electrons are transported through the reinforcement.

According to the results herein presented, the 2-electrode INESSCOM sensor can be reliably used for corrosion rate assessment of UHPFRC, despite its extremely high resistivity and, consequently, its very low i_{CORR} values.

3.2 | UHPFRC raft corrosion monitoring

This section shows the most interesting results for INESSCOM implementation in the offshore UHPFRC raft. Figures 9, 10 and 11 show the monitoring results obtained for the most important corrosion parameters over approximately 17 months. As seen in Figure 9a, the i_{CORR} value remains practically invariable within an extremely narrow range between 0.01 and 0.02 μA/cm^2 in the UHPFRC beams. These i_{CORR} values are very similar to those previously recorded in laboratory tests with the UHPFRC specimen (Figure 8a), as well as those obtained in other parallel studies aimed at verifying the reliability of different corrosion measurement techniques in UHPFRC.[35,36] Therefore, the corrosion process in UHPFRC beams can be explained using the same reasoning previously provided in Section 3.1.2. In any case, these i_{CORR} values are well below 0.1 μA/cm^2, which indicates negligible corrosion risk of the reinforcement; that is, it is in a passive state.[6,30]

Conversely, in the conventional concrete (CC) specimen, an increasing trend was observed in the i_{CORR} assessment (Figure 9a). Three different stages in the monitoring graph can be distinguished. Firstly, reinforcements remained in the passive state for more than 3 months (until day 100). Then a transitional period lasting around 100 days (between

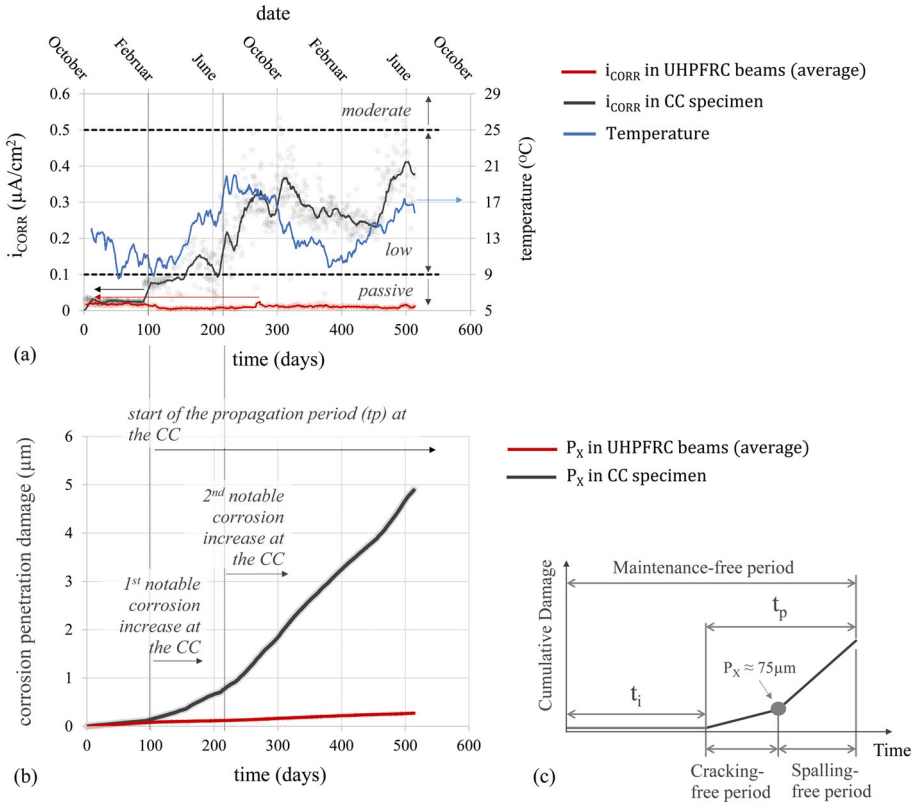

FIGURE 9 Corrosion rate results obtained after real-time monitoring the UHPFRC offshore raft for 17 months with the INESSCOM system: (a) temperature and corrosion current density (i_{CORR}); (b) corrosion penetration damage determined from the i_{CORR} values according to Equation (3); (c) simplified scheme for modelling the service life of corroding structures according to the Tutti model[8]

day 100 and 220) appeared, during which time steel was on the borderline between the passive and active state (around 0.1 μA/cm^2). For the remaining period (about 300 days), the corrosion level moved in the low-corrosion level zone, with an increasing trend towards the moderate-corrosion level zone. At the end of the period, the i_{CORR} of the CC specimen was approximately 0.4 μA/cm^2. This value was 40 times higher than that obtained for the UHPFRC beams.

These three stages observed in the i_{CORR} graph for the CC specimen were also distinguished on the graph in Figure 9b, which shows the corrosion penetration damage (P_X) obtained by integrating the monitored i_{CORR} values in Figure 9a over time according to[37]

$$P_X(\mu m) = 11.6 \cdot i_{CORR} \cdot t_p \quad (3)$$

This graph (Figure 9b) is particularly interesting because it can be compared with the Tutti diagram (Figure 9c), which is one of the most representative graphs of models that forecast service life. Although the UHPFRC beams remained within the initiation period (t_i), the CC specimen clearly exceeded this phase and entered the propagation period (t_p) from approximately 220 days. Despite the CC specimen clearly tended to move towards higher corrosion levels, the i_{CORR} value generally fluctuated in relation to cyclic changes in temperature (Figure 9a), hence the importance of monitoring temperature to facilitate i_{CORR} evolution interpretations.

According to some reference studies,[38] the first cracks could appear at $P_X \approx 75$ μm (Figure 9c), which fell short of the 5 μm estimated in the CC specimen (Figure 9b). However, the pitting factor α should be considered when

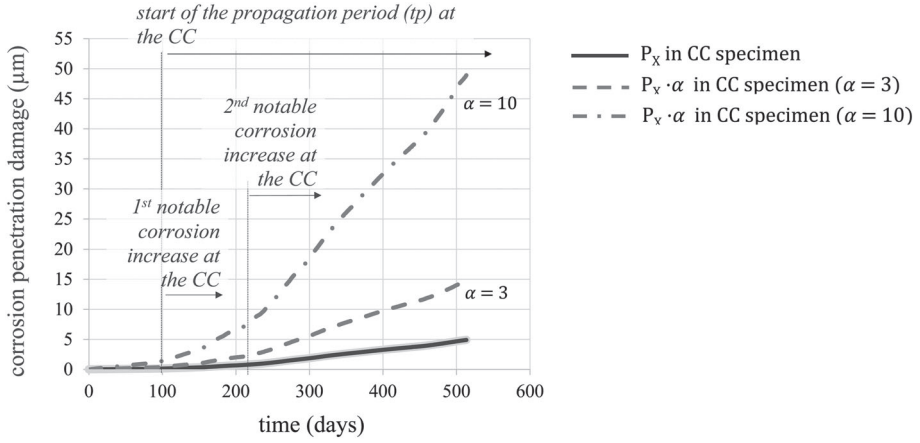

FIGURE 10 Corrosion penetration damage determined in the CC specimen with ($P_X \cdot \alpha$) and without (P_X) considering the pitting factor α. The most common two values for α depending on the pitting corrosion level assumed were considered, that is, α = 3 for several scattered and coarse pits and α = 10 for very localised pitting corrosion.

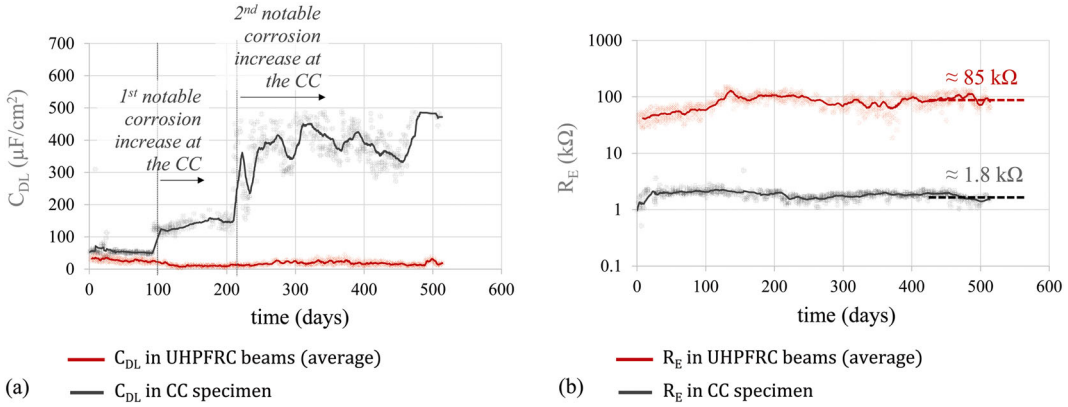

FIGURE 11 Evolution of additional corrosion parameters obtained after real-time monitoring the UHPFRC offshore raft for 17 months with the INESSCOM system: (a) double-layer capacity (C_{DL}); and (b) and electrical resistance of concrete (R_E)

determining the corrosion penetration damage,[39] whose value is equal to 2 for uniform corrosion and for localised corrosion may vary from 3 to 10.[6] The value of 10 applies to very localised pitting corrosion or to have conservative predictions.

Since chloride is assumed to be the main depassivating ion in the marine environment to which the raft is exposed, here, α would be between 3 and 10. As can be seen in Figure 10, the corrosion penetration damage estimated in the CC specimen is largely increased when applying $P_X \cdot \alpha$, reaching 50 μm with a clear increasing trend towards the end of the cracking-free period (≈75 μm) when $\alpha = 10$ is considered (very localised pitting corrosion) (Figure 9c).

Anyway, a realistic value of α will be obtained by analysing the real corrosion condition of the reinforcement when first cracks will appear in the CC specimen, which is not yet the case. Therefore, the change in slope seen in the graphs in Figures 9b and 10 would be related to variations in humidity and/or oxygen availability more than with external cracks appearing in concrete because of advanced rebar corrosion.

Figure 11 shows the evolution of the electrical resistance of concrete (R_E) and the double-layer capacity (C_{DL}), which are additional parameters of interest in corrosion monitoring and were obtained with the INESSCOM system according to the bases set out in previous research.[24,25] The C_{DL} trend in Figure 11a was very similar to that of the i_{CORR} (Figure 9a). This was expected bearing in mind that as corrosion increased, so did the amount of corrosion products (oxides) accumulated at the steel-concrete interphase which are known to behave as electrolytic capacitors.[40] Therefore, C_{DL} capacity increased, as evidenced in the CC specimen. A clear differentiation was observed for R_E (Figure 11b) between the specimen and raft beams, the UHPFRC reaching values approximately 47-fold higher than those in the CC. This was due to high UHPFRC compactness (low porosity), which made water penetration through pores extremely difficult, and also substantially limited chloride diffusion to rebars, which were completely protected from corrosion, at least during the analysed period (Figure 9a).

4 | CONCLUSIONS

The present work aimed to demonstrate the usefulness of the INESSCOM system to monitor corrosion processes in floating UHPFRC structures under service conditions. It is an autonomous sensor system for remote and real-time monitor several areas of a structure using an embedded sensor in which an innovative approach with potential step voltammetry (PSV) provides the corrosion rate (i_{CORR}) along with additional information such as electrical resistance of concrete (R_E), double layer capacity (C_{DL}) and temperature. Apart from that, the main sensor innovation lies in the use of a robust two-electrode measuring cell intended to ensure high reliability and durability. This sensor is composed of a carbon steel bar as working electrode (WE) and the reinforcement itself as counter-electrode (CE). The results obtained from previous laboratory tests using conventional concrete and UHPFRC specimens while monitoring an UHPFRC offshore raft allowed the following conclusions to be drawn:

1. The sensor's two-electrode measuring cell allowed the PSV technique to be satisfactorily applied to assess corrosion in concrete specimens with well-differentiated corrosion level. Two-electrode measurements tend to underestimate the corrosion current density (i_{CORR}) by about 20% with respect to the classic three-electrode measuring cell, which was generated for validation purposes by incorporating an embedded reference electrode into the two-electrode cell.
2. INESSCOM sensor provided accurate and reproducible corrosion rate measurements during the 5-months follow up of a UHPFRC specimen despite high resistivity (≈450 kΩ·cm) as a result of the material's excellent compactness (low porosity). i_{CORR} rapidly dropped at values of about 0.01 μA/cm^2, which were 4.5 times lower than those monitored in a conventional concrete sample with a w/c ratio of 0.6.
3. The UHPFRC offshore raft was successfully monitored by INESSCOM for 17 months. The i_{CORR} value remained well below the depassivation threshold of 0.1 μA/cm^2 throughout this period. Conversely, in the conventional concrete (CC) specimen with w/c ratio of 0.6 installed in the raft itself, the i_{CORR} value was around 0.4 μA/cm^2 (low corrosion) with an increasing trend towards the moderate-corrosion level zone. This active corrosion condition was attributed to rebar chloride depassivation.
4. Exhaustive i_{CORR} monitoring in the raft provided by INESSCOM allowed to obtain the corrosion penetration damage (μm) over time. This resulted in a monitoring diagram similar to the Tutti model, which was useful for accurately identifying the start of the propagation period and for estimating the end-of-service time of the structure. The UHPFRC raft beams were clearly remained within the initiation period, while the CC specimen reached the propagation phase where a change in corrosion kinetics due to a marked increase in corrosion rate was detected.

5. Consistent with corrosion rate results, the other parameters also showed well-differentiated trends in both concrete types in the raft. UHPFRC electrical resistance was generally around 47-times higher than that of the CC because of the material's excellent compactness, which strongly difficulted diffusion of depassivating agents. This would explain the extremely low corrosion rate values measured in the UHPFRC and, therefore, excellent durability attributed to UHPFRC as a structural building material.
6. INESSCOM has demonstrated to be a useful system in the structural health monitoring strategies adopted to assess the service life of concrete structures under very difficult conditions (marine environment, remote location, extremely high resistive concrete, etc.). The durability parameters provided by the monitoring system presented here may be highly useful in assessing the life cycle sustainability of innovative structural materials, such as the UHPFRC.

ACKNOWLEDGEMENTS

This work was supported by the pre-doctoral scholarship granted to Jose Enrique Ramon Zamora by the Spanish Ministry of Science and Innovation (grant number FPU13/00911). We wish to acknowledge financial support from the Spanish Ministry of Economy and Competitiveness through the National Programme of Oriented R&D&I to Societal Challenges (project numbers BIA2016-78460-C3-3-R, PID2020-119744RB-C21 and PID2020-119744RB-C22) and financial support from the UPV (project number SP20180245). We also appreciate the support provided by IETcc during part of the laboratory testing, especially Dr. Isabel Martinez Sierra, and by RDC and PREFFOR companies during on-site experimental work, especially Hugo Coll and Esteban Camacho.

AUTHOR CONTRIBUTIONS

José E. Ramón and **José M. Gandía-Romero:** sensors installation, investigation, writing-original draft, methodology, formal analysis. **Román Bataller:** sensors installation and electronic devices design and system communication. **Juan A. López:** pilot design and construction. **Juan Soto** and **Manuel Valcuende:** writing-reviewing and editing, supervision.

DATA AVAILABILITY STATEMENT

The data that support the findings of this study are available from the corresponding author upon reasonable request.

REFERENCES

1. Resplendino J, Toutlemonde F. *The UHPFRC revolution in structural design and construction*. In: RILEM-Fib-AFGC Int. Symposium on Ultra-High Performance Fibre-Reinforced Concrete, UHPFRC; 2013:791-804.
2. Azmee NM, Shafiq N. Ultra-high performance concrete: from fundamental to applications. *Case Stud Constr Mater*. 2018;9:e00197. doi:10.1016/j.cscm.2018.e00197
3. Wang W, Liu J, Agostini F, Davy CA, Skoczylas F, Corvez D. Durability of an ultra high performance fiber reinforced concrete (UHPFRC) under progressive aging. *Cem Concr Res*. 2014;55:1-13. doi:10.1016/j.cemconres.2013.09.008
4. Raupach M, Elsener B, Polder R, Mietz J. Corrosion of Reinforcement in Concrete: Mechanisms, Monitoring, Inhibitors and Rehabilitation Techniques (Woodhead publishing Vol 38); 2014. ISSN 1354-5116.
5. ASTM C876–15, Standard Test Method for Corrosion Potentials of Uncoated Reinforcing Steel in Concrete. West Conshohocken, PA, 2015.
6. Andrade C, Alonso C. Test methods for on-site corrosion rate measurement of steel reinforcement in concrete by means of the polarization resistance method. *Mater Struct*. 2004;37(9):623-643. doi:10.1007/BF02483292
7. EN 1992–1-1: Eurocode 2: Design of concrete structures—part 1-1: general rules and rules for buildings, CEN, 2015.
8. Tutti K. Corrosion of steel in concrete. *Swed Cem Concr Re. Inst* (Stockholm, Research Report FO 4); 1982. ISSN 0346-6906.
9. Figueira RB. Electrochemical sensors for monitoring the corrosion conditions of reinforced concrete structures: a review. *Appl Sci*. 2017; 7(11):1157. doi:10.3390/app7111157
10. Maruthapandian V, Saraswathy V, Muralidharan S. Development of solid state embeddable reference electrode for corrosion monitoring of steel in reinforced concrete structures. *Cem Concr Compos*. 2016;74:100-108. doi:10.1016/j.cemconcomp.2016.09.001
11. Elsener B. Macrocell corrosion of steel in concrete—implications for corrosion monitoring. *Cem Concr Compo*. 2002;24(1):65-72. doi:10.1016/S0958-9465(01)00027-0
12. Ramón JE, Gandía-Romero JM, Valcuende M, Bataller R. Integrated sensor network for monitoring steel corrosion in concrete structures. *VITRUVIO – Int J Archit Technol Sustain*. 2016;1(1):64-79. doi:10.4995/vitruvio-ijats.2016.5191
13. Gao J, Wu J, Li J, Zhao X. Monitoring of corrosion in reinforced concrete structure using Bragg grating sensing. *NDT E Int*. 2011;44(2): 202-205. doi:10.1016/j.ndteint.2010.11.011
14. Andringa MM, Neikirk DP, Dickerson NP, Wood SL. Unpowered wireless corrosion sensor for steel reinforced concrete. *SENSORS 2005 IEEE* 2005;4. doi:10.1109/ICSENS.2005.1597659.
15. Vélez W, Matta F, Ziehl P. Acoustic emission monitoring of early corrosion in prestressed concrete piles. *Struct Control Health Monit*. 2015;22(5):873-887. doi:10.1002/stc.1723

16. Moustafa A, Niri ED, Farhidzadeh A, Salamone S. Corrosion monitoring of post-tensioned concrete structures using fractal analysis of guided ultrasonic waves. *Struct Control Health Monit*. 2014;21(3):438-448. doi:10.1002/stc.1586
17. Martínez I, Andrade C. Examples of reinforcement corrosion monitoring by embedded sensors in concrete structures. *Cem Concr Compos*. 2009;31(8):545-554. doi:10.1016/j.cemconcomp.2009.05.007
18. Bernhard TJ, Hietpas K, George E, Kuchma D, Reis H. An interdisciplinary effort to develop a wireless embedded sensor system to monitor and assess corrosion in the tendons of prestressed concrete girders. *IEEE Top Conf Wirel Commun Technol*. 2003;2003:241-243. doi:10.1109/WCT.2003.1321506
19. Barsocchi P, Cassara P, Mavilia F, Pellegrini D. Sensing a city's state of health: structural monitoring system by internet-of-things wireless sensing devices. *IEEE Consum Electron Mag*. 2018;7(2):22-31. doi:10.1109/MCE.2017.2717198
20. Perez H, Tah JHM. Deep learning smartphone application for real-time detection of defects in buildings. *Struct Control Health Monit*. 2021;28(7):e2751. doi:10.1002/stc.2751
21. An Y, Chatzi E, Sim S-H, Laflamme S, Blachowski B, Ou J. Recent progress and future trends on damage identification methods for bridge structures. *Struct Control Health Monit*. 2019;26(10):e2416. doi:10.1002/stc.2416
22. Alcañiz M, Bataller R, Gandía-Romero JM, Ramón JE, Soto J, Valcuende M. Sensor, red de sensores, método y programa informático para determinar la corrosión en una estructura de hormigón armado, *invention patent No. ES2545669*, Publication date 19 January 2016.
23. Ramón JE. Sistema de Sensores Embebidos para Monitorizar la Corrosión en Estructuras de Hormigón Armado. Fundamentos, Metodología y Aplicaciones, PhD Thesis, Universitat Politècnica de València; 2018. doi:10.4995/Thesis/10251/111823.
24. Ramón JE, Martínez-Ibernón A, Gandía-Romero JM, et al. Characterization of electrochemical systems using potential step voltammetry. Part I: modeling by means of equivalent circuits. *Electrochim Acta*. 2019;323:134702. doi:10.1016/j.electacta.2019.134702
25. Ramón JE, Gandía-Romero JM, Bataller R, Alcañiz M, Valcuende M, Soto J. Potential step voltammetry: an approach to corrosion rate measurement of reinforcements in concrete. *Cem Concr Compos*. 2020;110:103590. doi:10.1016/j.cemconcomp.2020.103590
26. EN 206 2000. Concrete—Part 1: Specification, Performance, Production and Conformity. British Standards Institution, 2000.
27. Angst U, Büchler M. On the applicability of the Stern–Geary relationship to determine instantaneous corrosion rates in macro-cell corrosion. *Mater Corros*. 2015;66:1017-1028. doi:10.1002/maco.201407997
28. Warkus J, Raupach M. Numerical modelling of macrocells occurring during corrosion of steel in concrete. *Mater Corros*. 2008;59:122-130. doi:10.1002/maco.200804164
29. UNE 83988:2008 Spanish Standard, Concrete durability. Test methods. Determination of the electrical resistivity. Part 1: Direct test (reference method), 2008.
30. Berke NS, Chaker V, Whiting D. *Corrosion Rates of Steel in Concrete*. No. 1065. ASTM International; 1990.
31. Poursaee A, Hansson CM. Reinforcing steel passivation in mortar and pore solution. *Cem Concr Res*. 2007;37(7):1127-1133. doi:10.1016/j.cemconres.2007.04.005
32. Feliu S, González JA, Andrade C. Relationship between conductivity of concrete and corrosion of reinforcing bars. *Br Corros J*. 1989;24(3):195-198. doi:10.1179/000705989798270027
33. Hornbostel K, Larsen CK, Geiker MR. Relationship between concrete resistivity and corrosion rate—a literature review. *Cem Concr Compos*. 2013;39:60-72. doi:10.1016/j.cemconcomp.2013.03.019
34. Alonso MC, Soto J, Ferrara L, et al. Verification of durability of UHDCs under XA and XS accelerated tests. *ReSHEALience Consortium* Deliverable No. 5.1. Accessed June 30, 2019. https://ec.europa.eu/research/participants/documents/downloadPublic?documentIds=080166e5c5537ac6&appId=PPGMS
35. Soto J, Valcuende M, Gandía JM, et al. Verification of sensitivity and reliability of non-destructive methods and sensors. *ReSHEALience Consortium* Deliverable No. 5.2. Accessed October 31, 2019. https://ec.europa.eu/research/participants/documents/downloadPublic?documentIds=080166e5c8cd8121&appId=PPGMS
36. Valcuende M, Lliso-Ferrando JR, Ramón-Zamora JE, Soto J. Corrosion resistance of ultra-high performance fibre-reinforced concrete. *Construct Build Mater*. 2021;306:124914. doi:10.1016/j.conbuildmat.2021.124914
37. Andrade C. Propagation of reinforcement corrosion: principles, testing and modelling. *Mater Struct*. 2019;52(1):1-26. doi:10.1617/s11527-018-1301-1
38. Alonso C, Andrade C, Rodríguez J, Diez JM. Factors controlling cracking of concrete affected by reinforcement corrosion. *Mater Struct*. 1998;31(7):435-441. doi:10.1007/BF02480466
39. Andrade C, Alonso C, González JA, Rodríguez J. Remaining service life of corroding structures. *Durability of structures. IABSE Symposium* (Lisbon, report 57/1); 1989. 6–8.
40. González JA, Miranda JM, Otero E, Feliu S. Effect of electrochemically reactive rust layers on the corrosion of steel in a Ca (OH)2 solution. *Corros Sci*. 2007;49(2):436-448. doi:10.1016/j.corsci.2006.04.014

How to cite this article: Ramón JE, Gandía-Romero JM, Bataller R, López JA, Valcuende M, Soto J. Real-time corrosion monitoring of an ultra-high performance fibre-reinforced concrete offshore raft by using an autonomous sensor system. *Struct Control Health Monit*. 2022;e3102. doi:10.1002/stc.3102